Surfactant Micelles

DOI: 10.1002/ange.201406489

Monitoring the Transition from Spherical to Polymer-like Surfactant Micelles Using Small-Angle X-Ray Scattering**

Grethe Vestergaard Jensen, Reidar Lund, Jérémie Gummel, Theyencheri Narayanan, and Jan Skov Pedersen**

Abstract: *Despite over a century of modern surfactant science, the kinetic pathways of morphological transitions in micellar systems are still not well understood. This is mainly as a result of the lack of sufficiently fast methods that can capture the structural changes of such transitions. Herein, a simple surfactant system consisting of sodium dodecyl sulfate (SDS) in aqueous NaCl solutions is investigated. Combining synchrotron radiation small-angle X-ray scattering (SAXS) with fast stopped-flow mixing schemes allows monitoring the process where polymer-like micelles are formed from globular micelles when the salt concentration is suddenly increased. The results show that "worm-like" micelles are formed by fusion of globular micelles and short cylinders in a fashion that bears similarities to a step-like polymerization process.*

Since the discovery of "colloidal ions" about a century ago,[1] surfactant micelles has been a topic of continued intense interest in both academic and technological research. Surfactants have the ability to aggregate into a wide variety of interesting and highly dynamic nanostructures. They consist of a hydrophilic head group covalently linked to a hydrophobic tail (hydrocarbon) group. In aqueous solution above their critical micelle concentration (cmc) they self-assemble into micelles consisting of a hydrophobic core of tail groups surrounded by a shell of the hydrophilic head groups and water. The shape and size of the micelles depend on the type of surfactant and conditions, such as temperature and solvent composition. Since their discovery by McBain in 1913,[1] micelles with various nonspherical shapes, such as ellipsoidal, cylindrical, and discoidal, have been identified.[2,3] It is still interesting to obtain insight into the fundamental behavior of surfactant systems, because of the widespread applications ranging from basic technologies, such as detergents and additives in daily products to advanced applications in biotechnology and nanotechnologies.[4–7] Indeed, the surfactant market continues growing and is expected to grow even further to about $36 billion over the next years.[39]

One of the most extensively studied systems in the field of surfactant science is sodium dodecyl sulfate (SDS) micelles in aqueous solutions. The study of SDS and other classical surfactant systems is well-established.[5,6,8] The structure and phase behavior of SDS upon changing various conditions, such as salt, co-solvents, temperature, and pressure, are well-known.[9–12] Recent advances in computer power and algorithms have also allowed simulations[13] with atomic resolution that can reproduce very detailed aspects of the micelles including shape and critical micelle concentrations.[14,15]

Despite the impressive amount of data on surfactants in solution, much less is known about their dynamic behavior and non-equilibrium kinetics associated with morphological transitions. Previously, classical kinetics experiments were performed in the linear region by slightly perturbing surfactant solutions and monitoring the relaxation back to equilibrium.[16] The results show that the relaxation pattern for typical charged surfactants can be described by two rate constants whereas systems with screened electrostatic interactions or neutral surfactants follow a more complicated relaxation pattern that depends significantly on several conditions, such as concentration and salt content.[17,18]

Micelle kinetics have been measured under conditions further away from equilibrium using modern time-resolved small-angle neutron scattering (TR-SANS)[19–22] and small-angle X-ray scattering (TR-SAXS).[23–26] In contrast to other techniques, TR-SAXS/TR-SANS is able to capture the structural evolution on the order of milliseconds. Herein, we show that the transition from individual globular micelles to worm-like micelles can be followed using a combination of time-resolved SAXS and stopped-flow experiments working in a stroboscopic mode. Interestingly, the transition bears some similarities to step-like polymerization reactions as individual spheres are consumed rapidly and added to existing multimers, forming eventually long flexible cylinders, that is, polymer-like micelles ("worms") through consecutive fusion processes. For a system having a lower amount of NaCl, the residual electrostatic interactions prevent fusion and only slightly elongated prolate ellipsoids are formed.

For SDS dissolved in pure water, the negative charge of the anionic head group results in a high degree of electrostatic repulsion between the head groups in the micelle. This leads to a large effective head-group area and a high curvature of

[*] Dr. G. V. Jensen, Prof. J. S. Pedersen
Department of Chemistry
and Interdisciplinary Nanoscience Center (iNANO)
Aarhus University, Gustav Wieds Vej 14, 8000 Aarhus C (Denmark)
E-mail: jsp@chem.au.dk

Dr. R. Lund
Dept. of Chemistry, University of Oslo
Postboks 1033 Blindern, 0315 Oslo (Norway)
E-mail: reidar.lund@kjemi.uio.no

Dr. J. Gummel, Dr. T. Narayanan
European Synchrotron Radiation Facility (ESRF)
71 Avenue des Martyrs, 38043 Grenoble Cedex (France)

[**] We are indebted to the European Synchrotron Radiation Facility (ESRF) for providing beam time. R.L. greatly acknowledges grants from the Norwegian Research Council, under the SYNKNOYT program (218411 and 228573).

Supporting information for this article is available on the WWW under http://dx.doi.org/10.1002/anie.201406489.

the micelle core and, consequently, formation of globular micelles. When the ionic strength of the solvent is increased, the effective head-group area decreases, and at a certain point, cylindrical micelles are formed. Classically, this can be roughly interpreted in terms of a change in the packing parameter, defined as $p = v_0/a_0 l$, where v_0 and l are the surfactant tail volume and length, respectively, and a_0 is the head-group area. In general, an approximate p value of $p = 1/3$ favors spheres, whereas values closer to $p = 1/2$ lead to cylinder formation. Thus, decreasing the effective area of the head group as a result of attraction or less electrostatic repulsion would lead to a larger p value driving the transformation. This is also seen in simulations.[13] This transition from globular to long worm-like micelles driven by the addition of salt is illustrated in Figure 1 a.

Figure 1 b shows the scattering data corresponding to the initial and final solutions, respectively, for the system investigated. The scattering intensity in absolute units is plotted against the modulus of the scattering momentum transfer Q, defined as $Q = 4\pi\sin(\theta)/\lambda$, where 2θ and λ are the scattering angle and wavelength, respectively. This data is measured for the initial SDS solutions in pure water and after mixing a solution of SDS (1 wt %; wt = weight) in a 1:1 ratio with either a 1 M or a 2 M NaCl solution, respectively, to produce final solutions with NaCl concentrations of 0.5 M and 1 M NaCl, respectively. For the unmixed SDS solution, the intensity decreases towards the lowest Q value and the tendency is more pronounced for higher concentrations. This can be attributed to the electrostatic repulsions between the micelles and the associated structure factor effects.[27] The data can be well-described using a model of ellipsoidal core–shell particles including a Hayter and Penfold structure factor $S(Q)$ to account for the effect of the screened Coulomb repulsion.[28,29] The obtained structural parameters (see Supporting Information) are in good agreement with reported values.[11]

For the SDS–salt solutions, quite different behavior is measured, in particular at low Q values. While the data recorded in 0.5 M NaCl solution exhibit an almost constant, plateau-like scattering, indicating globular micelles of limited size, there is a significant upturn at low Q values for the 1 M NaCl solution, demonstrating the elongation/growth of the micelles as an effect of the electrostatic screening. For the 0.5 M NaCl solution, the fits show the presence of slightly larger ellipsoidal micelles with a core radius $R_{core,ell} = (16.0 \pm 0.2)$ Å, corresponding very well with the length of a stretched C_{12} tail,[30] whereas the aspect ratio is $\varepsilon = 1.95 \pm 0.07$, and the head-group shell thickness is $D = 7.3 \pm 0.2$ Å. No sign of repulsion between micelles is present in the scattering pattern, and thus a structure factor was not included in the model. It should be mentioned that oblate micelles ($\varepsilon < 1$) could in some cases fit the data equally well.[12,31–33] However, given the tendency for elongation in solutions of higher salt concentration, we considered prolate micelles as being most reasonable.[32] In any case, we expect both types of ellipsoids to be present because of the expected strong fluctuations of the micelle. However, this cannot be readily distinguished using (static) scattering techniques.

For 1 M NaCl solutions, the data can be best described with a core–shell model for long cylindrical micelles. However, the data show clear sign of a finite flexibility, which is indicated by an upturn at low Q values relative to the Q^{-1} behavior of straight rods. This is clearly seen in Figure 1 b, where the calculated line for a straight cylinder clearly falls below the fits that include a polymer-like flexibility at low Q values. Using a fit model for these worm-like micelles (Supporting Information), a Kuhn length, b, of 580 Å was obtained. The overall contour length is outside the resolution of the SAXS experiment, and it was set to an arbitrary value of 1000 Å. The cross section of the worms was found to have a core radius of $R_{core,w} = 15.0$ Å and a shell thickness of $D = 8$ Å.

To investigate the kinetics of the transition from spherical to elongated micelles, pure SDS solutions were rapidly mixed with NaCl solutions using a stopped-flow apparatus (SFA) and then followed by TR-SAXS. The kinetics were generally too fast for regular sampling using frames with 140 ms delays (set by the minimal detector read-out time). To obtain higher time resolution, a stroboscopic approach was used where the measurements were systematically repeated, varying the

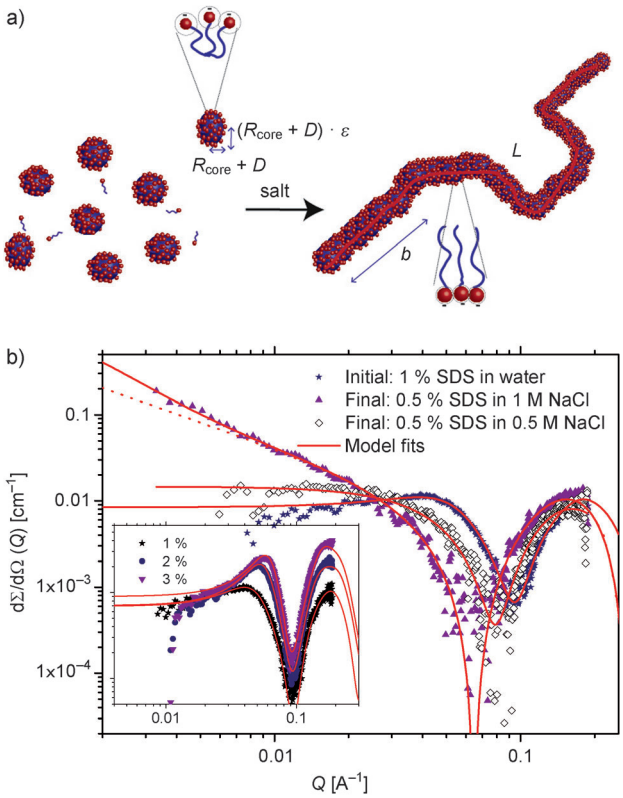

Figure 1. a) Schematic representation of the transition from globular to long flexible cylindrical (worm-like) micelles. The transition is driven by decreased electrostatic head-group repulsions upon addition of salt. b) SAXS data showing the absolute scattering intensity plotted against the modulus of the scattering momentum (Q) for the initial SDS solution and the mixtures with NaCl corresponding to the final states. Inset: the concentration dependence of the pure SDS solution (at concentrations 1, 2, and 3 wt %) in water. Solid lines: data fits by core–shell models of ellipsoids or worm-like cylinders. Dotted line: fit of the data to the theoretical scattering behavior at low Q values for a perfectly straight cylinder, indicating the excess scattering at low Q values that can be attributed to the finite flexibility of the chains. R_{core} = core radius; D = shell thickness; ε = aspect ratio; b = Kuhn length; L = average length.

delay from mixing to collection of the first frame. This requires complete reproducibility of the mixing, which was found to be the case. Using this method, the dead time between frames was decreased to a few milliseconds.

Figure 2 shows examples of data obtained from such kinetic runs, depicting structural evolution of SDS solutions (1 wt%) after mixing with equal amounts of NaCl solution of either a) 1 M, or b) 2 M concentration, to produce final solutions of 0.5 M and 1 M NaCl, respectively. Data for alternative concentrations of SDS samples (0.5 and 1.5 wt%) are shown in the Supporting Information. The kinetic data frames for $c_{NaCl} = 0.5$ M are perfectly described by ellipsoidal core–shell particles at all time frames. However, there is a clear increase in the intensity that is accompanied with a less pronounced minimum in the scattering data. This indicates growth and some elongation. Optimized $R_{core,ell}$ values close to 16.6 Å were obtained. This corresponds to the length of a stretched C_{12} tail,[30] and the $R_{core,ell}$ value was fixed at this value for all kinetic frames. The fit parameters for the time dependence of the core aspect ratio (ε) resulting from the fits are plotted in Figure 3 a.

The shell thickness contracts slightly from about 8 to 7 Å (see the Supporting Information) and the aspect ratio increases significantly within the time period $t = 10$–30 ms. When the $R_{core,ell}$ value is held constant, the aggregation number (average number of molecules per micelle) is proportional to the aspect ratio ε. Interestingly, the growth behavior can be described by a simple exponential growth model ($\varepsilon \approx 1 - \exp(-t/\tau)$), characterized by a single time constant τ. The data suggest a slight concentration dependence with $\tau = 23 \pm 5$ ms and $\tau = 19 \pm 3$ ms for the lowest and the highest SDS concentration, respectively. For equilibration through stepwise insertion/expulsion of single surfactant molecules, the relaxation time is expected to increase with the surfactant concentration.[34–36] Thus, this mechanism seems not to be dominant in the kinetic process.

For the 1 M NaCl system, a more pronounced increase in intensity with time is measured, associated with an increasingly negative slope at low Q values, reflecting a transition to long worm-like micelles. These data can best be described using a linear combination of ellipsoidal and worm-like micelles, where the worm-like micelles consist of a fraction of the SDS molecules, $\phi_{worm} = 1 - \phi_{ell}$, where ϕ_{ell} is the corresponding fraction of the ellipsoidal micelles. To take into account a finite polydispersity in length of the worm-like micelles, we assumed an exponential distribution expected for such micelles of average length L_{ave} at equilibrium.[37] For the model fits, the shell thickness was fixed at $D = 8$ Å as this value gave good fits for both the initial ellipsoidal micelles

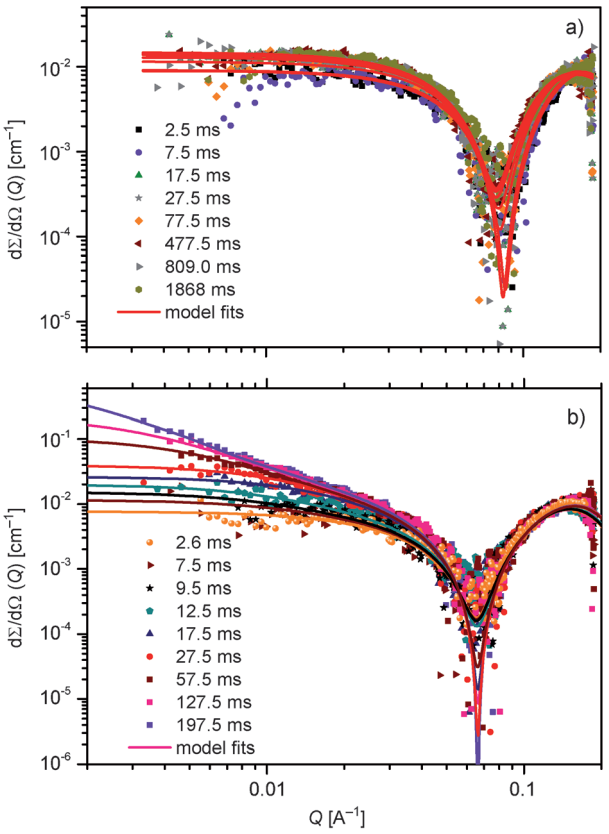

Figure 2. Time-dependent scattered intensity obtained using stopped-flow apparatus combined with a stroboscopic measurement system, plotting absolute scattering intensity against the modulus of the scattering momentum (Q). Data obtained after mixing a solution of SDS (1%) with a) 1 M NaCl and b) 2 M NaCl solutions. Solid lines: fits to the data of the ellipsoidal core–shell model (a) and worm-like core–shell model (b).

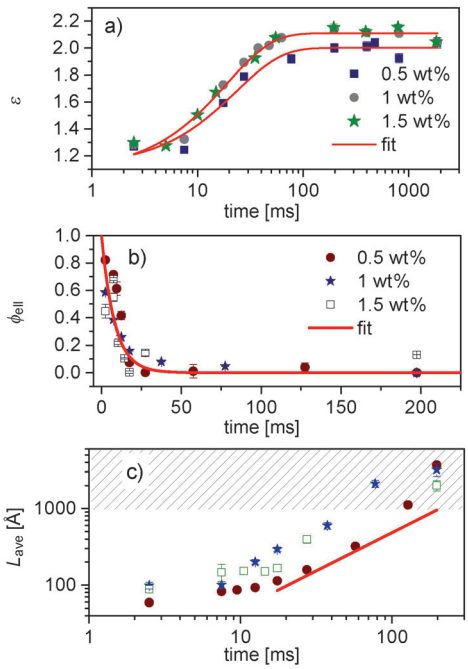

Figure 3. Fit parameters obtained from the experimental kinetic data, measured for different SDS concentrations (0.5, 1, and 1.5 wt%). a) Time dependence of the aspect ratio (ε) measured for SDS in NaCl solution (0.5 M). Solid lines: fit to the data of an exponential growth model. b) Time dependence of the fraction of spherical (ellipsoidal) micelles (ϕ_{ell}) measured for SDS in NaCl solution (1 M). c) Evolution of the contour length (L_{ave}) with time of the worm-like micelles measured for SDS in NaCl solution (1 M). Note: legend as in (b). Solid line: linear time dependence ($L_{ave} \approx t$). Hatched area indicates lengths beyond 1000 Å, which is the limit of the structural resolution.

and the final worm-like micelles. For the final frames where the worm-like micelles dominate, a core radius close to $R_{core,w} = 15.0$ Å is obtained. Thus, the $R_{core,w}$ value was fixed at this value for each of the kinetic frames. The ellipsoid core radius was again fixed at $R_{core,ell} = 16.6$ Å, whereas the axis ratio was fixed to $\varepsilon = 1.5$. The Kuhn length, b, was fixed at the value obtained from a fit to the final frame, where scattering from worm-like micelles dominate. Specifically, b values of 585 Å ($c = 0.5$ wt %), 747 Å ($c = 1$ wt %), and 800 Å ($c = 1.5$ wt %) were employed, in which the b value for the highest concentration approaches the maximum size resolution of the experiment. Note, it is only when the contour length of the micelle, L_{ave}, exceeds the value of b, that the micelles display a worm-like character.

The optimized values for the fraction of the ellipsoidal micelles ϕ_{ell} and the average length L_{ave} are plotted in Figures 3b and 3c, respectively. The fraction of ellipsoids ϕ_{ell} decreases rapidly, approximately following a simple single exponential decay, $\phi_{ell}(t) \approx \exp(-t/\tau_E)$, with a time constant of about $\tau_E = 10$ ms. The determined τ_E values do not show a strong concentration dependence.

The contour length of the worm-like micelles seems to depend significantly on concentration where the growth in length occurs more rapidly with increasing concentration from 0.5 % to 1 % (Figure 3c). Intriguingly, at longer times, the data show a pronounced tendency towards linear behavior in a double logarithmic plot, suggesting a power law growth $L_{ave} \approx t^x$. In fact as indicated by the solid line in Figure 3c, the time dependence corresponds well with a linear law $L_{ave} \approx t$. Although not directly related, such dependency is also measured for externally catalyzed stepwise growth polymerization reactions (e.g. acid-catalyzed condensation polymers) where a linear relationship between mean molecular weight and time is observed.[38] In such reactions the polymers grow in a stepwise manner through addition reactions involving the end groups, hence monomers are consumed rapidly and polymeric growth occurs through a combination of oligomers rather than by continuously adding monomers. In this way, this growth mechanism bears certain similarities to the mechanism of growth for the present worm-like (polymeric) micelles. Hence, this finding suggests that individual micelles undergo successive fusion events resulting in elongated structures. As a result of the high curvature, the surface energy is highest at the end of the cylinder and thus fusion events here may have higher probability, which may explain the similarity to step–growth polymerization kinetics. However, it should be mentioned that the same kinetic mechanism would predict that $1/\phi_{ell}(t) \approx t$, which is not observed. Nevertheless, it is clear from the pronounced concentration dependence that fusion events play a prominent role and that the overall growth appears to be linear and thus resembles a step–growth polymerization process. It is obvious from the pronounced difference between the kinetics in NaCl solutions of different concentrations (0.5 and 1 M) that the electrostatic interactions play a decisive role in the kinetics. It is likely that in 1 M NaCl solution most of the repulsion is screened, facilitating fusion of micelles, whereas in 0.5 M NaCl solution residual repulsions only allow growth through mainly molecular exchange mechanisms. A schematic drawing showing the proposed mechanism is given in Figure 4.

In conclusion, by employing time-resolved/stroboscopic SAXS we have successfully observed the formation of worm-like/polymer-like micelles from globular micelles. Through a quantitative analysis, we deduce that the kinetic pathway of formation involves successive fusion events. Furthermore, we find an almost linear time dependence of the micellar length which may suggest that the kinetics of formation resemble that commonly found for stepwise polymerization processes. This direct observation of this process and the quantitative determination of its kinetics have not been investigated to date. The identification of a polymer-type growth process in surfactant solutions provides an interesting contribution to the understanding of non-equilibrium processes in soft matter in general, giving a unique insight which is important both for fundamental and technological research.

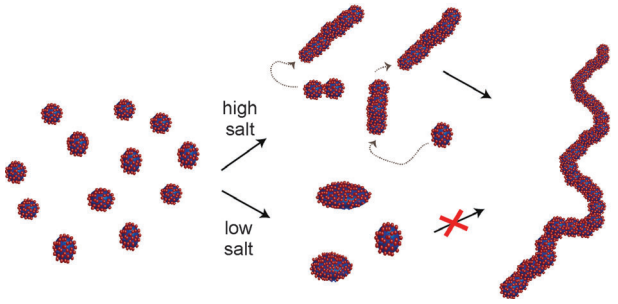

Figure 4. Schematic representation of the transition from spherical/ellipsoidal micelles to polymer-like micelles.

Received: June 23, 2014
Revised: July 17, 2014
Published online: September 4, 2014

Keywords: kinetics · micelles · small-angle X-ray scattering · step–growth polymerization · surfactants

[1] J. W. McBain, *Trans Faraday Soc.* **1913**, *9*, 93.
[2] M. Bergström, J. S. Pedersen, *J. Phys. Chem. B* **1999**, *103*, 8502.
[3] C. Wang, Z. Wang, X. Zhang, *Acc. Chem. Res.* **2012**, *45*, 608.
[4] M. Moradi, Y. Yamini, *J. Sep. Sci.* **2012**, *35*, 2319.
[5] D. Attwood, A. T. Florence, *Surfactant Systems, Their Chemistry, Pharmacy and Biology*, Chapman and Hall, New York, **1983**.
[6] T. F. Tadros, *Applied Surfactants: Principles and Applications*, Wiley, Hoboken, **2006**.
[7] J. D. Van Hamme, A. Singh, O. P. Ward, *Biotechnology Advances, Vol. 24*, Elsevier, Amsterdam, **2006**, p. 604.
[8] B. Jönsson, B. Lindman, K. Holmberg, B. Kronberg, *Surfactants and Polymers in Aqueous Solution*, Wiley, New York, **2000**.
[9] S. Vass, T. Gilányi, S. Borbély, *J. Phys. Chem. B* **2000**, *104*, 2073.
[10] S. Vass, T. Torok, G. Jakli, E. Berecz, *J. Phys. Chem.* **1989**, *93*, 6553.
[11] L. Arleth, M. Bergström, J. S. Pedersen, *Langmuir* **2002**, *18*, 5343.
[12] M. Bergström, S. J. Pedersen, *Phys. Chem. Chem. Phys.* **1999**, *1*, 4437.

[13] A. Jusufi, A.-P. Hynninen, M. Haataja, A. Z. Panagiotopoulos, *J. Phys. Chem. B* **2009**, *113*, 6314.
[14] M. Sammalkorpi, M. Karttunen, M. Haataja, *J. Phys. Chem. B* **2009**, *113*, 5863.
[15] F. Palazzesi, M. Calvaresi, F. Zerbetto, *Soft Matter* **2011**, *7*, 9148.
[16] E. Aniansson, S. N. Wall, M. Almgren, H. Hoffmann, I. Kielmann, W. Ulbricht, R. Zana, J. Lang, C. Tondre, *J. Phys. Chem.* **1976**, *80*, 905.
[17] E. Lessner, M. Teubner, M. Kahlweit, *J. Phys. Chem.* **1981**, *85*, 1529.
[18] E. Lessner, M. Teubner, M. Kahlweit, *J. Phys. Chem.* **1981**, *85*, 3167.
[19] S. U. Egelhaaf, *Curr. Opin. Colloid Interface Sci.* **1998**, *3*, 608.
[20] R. Lund, L. Willner, D. Richter, *Advances in Polymer Science*, *Vol. 259*, Springer, Berlin, **2013**, p. 51.
[21] R. Lund, L. Willner, D. Richter, P. Lindner, T. Narayanan, *ACS Macro Lett.* **2013**, *2*, 1082.
[22] G. V. Jensen, R. Lund, J. Gummel, M. Monkenbusch, T. Narayanan, J. S. Pedersen, *J. Am. Chem. Soc.* **2013**, *135*, 7214.
[23] R. Lund, L. Willner, M. Monkenbusch, P. Panine, T. Narayanan, J. Colmenero, D. Richter, *Phys. Rev. Lett.* **2009**, *102*, 188301.
[24] T. Narayanan, *Curr. Opin. Colloid Interface Sci.* **2009**, *14*, 409.
[25] T. Narayanan, J. Gummel, M. Gradzielski, *Advances in Planar Lipid Bilayers and Liposomes*, *Vol. 20*, Elsevier, **2014**, p. 171.
[26] S. Schmölzer, D. Gräbner, M. Gradzielski, T. Narayanan, *Phys. Rev. Lett.* **2002**, *88*, 258301.
[27] J. S. Pedersen in *Soft Matter Characterization* (Eds.: R. Borsali, R. Pecora), Springer, Dodrecht, **2008**, p. 191.
[28] J. B. Hayter, J. Penfold, *Mol. Phys.* **1981**, *42*, 109.
[29] J.-P. Hansen, J. B. Hayter, *Mol. Phys.* **1982**, *46*, 651.
[30] C. Tanford, *The Hydrophobic Effect: Formation of Micelles and Biological Membranes*, 2ednd edWiley, New York, **1980**.
[31] P. A. Hassan, G. Fritz, E. W. Kaler, *J. Colloid Interface Sci.* **2003**, *257*, 154.
[32] S. Vass, J. S. Pedersen, J. Pleštil, P. Laggner, E. Rétfalvi, I. Varga, T. Gilányi, *Langmuir* **2008**, *24*, 408.
[33] B. J. Hammouda, *J. Res. Natl. Inst. Stand. Technol.* **2013**, *118*, 151.
[34] E. A. G. Aniansson, S. N. Wall, *J. Phys. Chem.* **1974**, *78*, 1024.
[35] E. A. G. Aniansson, S. N. Wall, *J. Phys. Chem.* **1975**, *79*, 857.
[36] E. A. G. Aniansson, S. N. Wall, M. Almgren, H. Hoffmann, I. Kielmann, W. Ulbricht, R. Zana, J. Lang, C. Tondre, *J. Phys. Chem.* **1976**, *80*, 905.
[37] M. E. Cates, S. J. Candau, *J. Phys. Condens. Matter* **1990**, *2*, 6869.
[38] P. J. Flory, *Principles of Polymer Chemistry*, Cornell University Press, New York, **1953**.
[39] http://www.marketsandmarkets.com/Market-Reports/biosurfactants-market-493.html.

